EVOLUTION IN ELECTRICAL AND ELECTRONIC ENGINEERING
e-ISSN: 2756-8458

EEEE

Vol. 5 No. 1 (2024) 497-503
https://publisher.uthm.edu.my/periodicals/index.php/eeee

Effect of Seeding Time in the Formation of Gold Nanobipyramids Toward Glucose Detection

Syazwani Sukelan[1], Marlia Morsin[1,2]*, Natasya Salsabiila[1,2], Nur Liyana Razali[1,2]

[1] *Faculty of Electrical and Electronic Engineering*
Universiti Tun Hussein Onn Malaysia, Batu Pahat, 86400, Johor, MALAYSIA

[2] *Microelectronics & Nanotechnology –Shamsuddin Research Centre (MiNT-SRC),*
Institute for Integrated Engineering,
Universiti Tun Hussein Onn Malaysia, Batu Pahat, 86400, Johor, MALAYSIA

*Corresponding Author: marlia@uthm.edu.my
DOI: https://doi.org/10.30880/eeee.2024.05.01.062

Article Info

Received: 10 January 2024
Accepted: 12 March 2024
Available online: 30 April 2024

Keywords

Gold nanobipyramids, seeding time, plasmonic sensor, seed-mediated growth method

Abstract

This study explores the impact of varying seeding times on the formation of gold nanobipyramids (GNBPs) for glucose detection. The synthesis of GNBPs employs the seed-mediated growth method (SMGM), with seeding time ranging from 30 minutes to 3 hours. The investigation includes detailed UV-Vis and FESEM characterizations to study the optical and morphological properties of GNBPs. The optical characterization shows the seeding of GNBPs exhibited transverse Surface Plasmon Resonance (t-SPR) peaks around 300 to 400 nm, indicating higher presence of decahedral impurity while growth of GNBPs exhibited t-SPR peaks around 550 to 600 nm indicates the diameter of GNBPs and longitudinal Surface Plasmon Resonance (l-SPR) peaks around 850 to 950 nm linked to their aspect ratio of nanoparticles. However, the surface density of GNBPs ranged from 12.26 ± 3.729 % to 62.35 ± 12.17 %, with aspect ratios between 2.61 ± 0.067 and 3.27 ± 0.243. The optimum seeding time to synthesize GNBPs is 2 hours and proceeded into a sensing material for glucose detection through a plasmonic sensor. The plasmonic sensor is successfully developed with good stability for 600 seconds of non-stop measurement due to t-SPR and l-SPR, which exhibit consistent intensity changes over time for both bands.

1. Introduction

Over the past decade, there has been a growing emphasis on the unique electronic and chemical attributes of gold and silver as noble metals within the realm of nanotechnological research [1]. Existing literature delves into a comprehensive exploration of gold and silver due to their nanoparticle structures and sizes. Gold nanoparticles (GNPs), distinguished by their varied morphologies, including spherical, octahedral, icosahedral, multiple twinned, decahedral, tetrahedral, nanotriangles, hexagonal, plates, nanorods, and nanobipyramids, have gained prominence in biotechnology due to their larger surface area and superior conductivity compared to silver [2], [3]. GNPs emerge as key players in smart sensing devices, leveraging strong electric field characteristics, serving diagnostic purposes in biotechnology and medical applications [4]. Also, GNPs can be used for organic photovoltaics, sensor probes, therapeutic agents, drug delivery, electronic conductors, and catalysis [5]. Gold

nanoparticles with bipyramids shape, or gold nanobipyramids (GNBPs) for glucose detection-based plasmonic sensors with their properties will be discussed in this study. Other researchers employed GNBPs as the main nanosensor with various applications, such as Jin et al., explore the application of GNBPs for cancer therapy through the enhancement of the O_2 generation and hyperthermia [6]. Another work Suratun Nafisah et al. reported uses GNBPs as sensing materials to improve sensitivity and selectivity toward glyphosate detection-based plasmonic sensors [7].

Plasmonic sensors, leveraging the optical phenomenon known as Localized Surface Plasmon Resonance (LSPR), exhibit two distinct LSPR bands corresponding to the longitudinal and transverse electron oscillations associated with GNBPs. These inherent characteristics allow GNBPs to have heightened refractive index sensitivity (RIS) and an improved Figure of Merit (FOM) value, thereby enhancing sensing sensitivity [8]. This enhancement stands in stark contrast to conventional bulk metal thin film-based Surface Plasmon Resonance (SPR) sensors [9], with the degree of improvement contingent upon the nanoscale dimensions of the particles [10]. Consequently, the optical properties of GNBPs render them particularly advantageous for the development of plasmonic sensors, positioning them as great candidates among metal nanoparticles for sensing applications [11].

One critical parameter influencing the characteristics of GNBPs is the seeding time, a determinant of the shape and size of the sensing material. For instance, Marlia *et al.* investigated 1 hour to 3 hours of seeding time to observe its impact on the formation of gold nanoplates[12]. Similarly, Zehan *et al.* explored a range from 30 minutes to 24 hours for the growth time in the formation of gold nanorods[13]. The investigation of seeding time affects the aspect ratio, density, and size shape of nanoparticles, which necessitates determining the optimal time for GNP. Also, the reactive agent influences the seeding affects the growth of gold nanoparticles such as cetyltrimethylammonium bromide (CTAB) as a surfactant agent enhances the creation of GNP in the presence, which involves the basis of the synthesis to form elongated nanobipyramids structure with smooth surface of nanoparticle [16], [25]. This phenomenon suggests that increased GNBP formation reduces aggregation extent, resulting in a slower reduction in GNBP intensity. The positive ionic charge micelles formed by CTAB surrounding GNBPs prevent their aggregation, confirming the quantity of GNBPs plays a crucial role in maintaining optical properties. Ascorbic acid another reduction agent, acts more slowly leading to incomplete reduction of Au^{3+} to Au and consequently reducing the formation of GNBPs [7]. This underscores the significance of determining an optimum temporal parameter for the seeding process, considering its consequential effects on the morphological and dimensional characteristics of the nanoparticles.

The primary objective of this study is to examine the influence of seeding time on the formation of GNBPs for glucose detection applications. Glucose, a sugar derived from various sources such as food, humans, and plants[14], holds paramount significance in numerous biological processes essential for the synthesis of biomolecules. Classified as a monosaccharide, glucose is a pivotal type of carbohydrate, alongside other sugars such as fructose, galactose, ribose, and lactose. Its molecular formula is represented by $C_6H_{12}O_6$ [15]. This research delves into the relationship between seeding time and the resultant GNBPs for effective glucose-sensing applications because the morphology of GNBPs has two sharps end tips that contribute larger electron density and improve the local electric field that has a better practical application [26]. Moreover, seed-mediated growth is preferred for the synthesis of GNBPs in smaller sizes, low cost, and higher yield.

2. Methodology

GNBPs are synthesized by using the Seed-Mediated Growth method (SMGM) with different seeding time [7]. The fabrication of GNBPs encompasses two pivotal phases: the seeding and growth processes. The seeding solution is prepared by mixing 9.75 mL of 0.1 M cetyltrimethylammonium bromide (CTAB) with 0.15 mL of 0.01 M gold (III) chloride, 0.1 mL of 0.1 M chloroplatinic acid, and adding 0.9 mL of 0.01 M ice-cooled sodium borohydride into the solution. The seeding process is then replicated at distinct intervals, specifically at 30 minutes, 1 hour, 2 hours, and 3 hours, as part of a systematic investigation.

The growth solution involved mixing 20 mL of 0.1 M CTAB with 0.875 mL of 0.01 M gold (III) chloride, 0.025 mL of 0.01 M chloroplatinic acid, 0.2 mL of 0.01 M silver nitrate, 0.4 mL of 1 M hydrochloric acid, and 0.16 mL of 0.1 M ascorbic acid. Subsequently, the colour of the solution undergoes a transformation from yellow to colourless. Following this, 0.05 mL of each seeding solution is introduced, leading to a further change in colour progression from colourless to purple hue in 2 hours.

After that, the samples are centrifuged for three cycles. This process using a German Eppendorf centrifuge machine model 5804 operating at 5000 rpm, with each cycle lasting 60 minutes. Then, the pure GNBPs proceeded into Ultra Violet – Visible (UV-Vis) and Field Emission Scanning Electron Microscopy (FESEM) techniques by dropping on an indium tin oxide (ITO) substrate.

The setup of the plasmonic sensor involves the integration of five primary components involves a light source, a sensor chamber, a fiber optic, a spectrometer, and a computer equipped with OceanView software. The sensor chamber is designed to place the solution containing sensing material and glucose as a targeted analyte. The fiber optic serves as a transmission medium, establishing a connection between the light source, sensor chamber, and

spectrometer. Subsequently, the sensor undergoes testing, focusing on its stability and selectivity, crucial aspects in evaluating its performance and efficacy for glucose detection.

3. Result and Discussion

The SMGM employed in this study comprises two distinct stages: the seeding process and the growth process. The seeding process assumes a pivotal role in shaping the quality of the resultant GNBPs within the solution. This investigation delves into four different durations for the seeding process, namely 30 minutes, 1 hour, 2 hours, and 3 hours. The variations in seeding time are systematically examined to discern their impact on the characteristics and attributes of the grown GNBPs.

Two primary techniques, namely UV-Vis and FESEM, are conducted on the samples to analyze the GNBPs properties comprehensively. Post the seeding process as depicted in Fig. 1 (a), the presence transformed from colourless to a brownish hue. Subsequently, Fig. 1 (b) the growth process manifested in a shift from the initial purple colour. The presence of this purple hue signifies the successful formation of GNBPs strongly supported by Guo *et al*. that the appearance of a purple colour serves to the formation of GNBPs and their by-product. Thus, different shades are attributed to the influence of distinct shapes, sizes, or densities inherent in the obtained GNBPs [24].

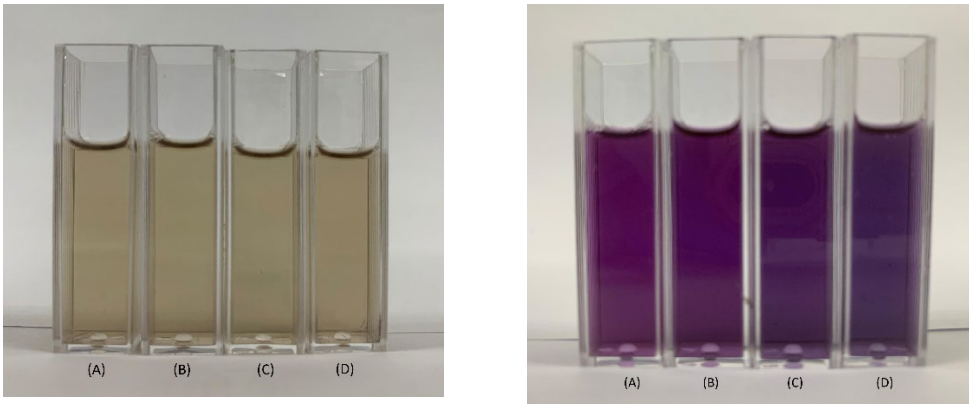

(a) (b)

Fig.1 *The growth solution with different seeding time. Sample A to D indicates 0.5-hour, 1-hour, 2-hour, and 3-hour. (a) The presence of seeding process (b) The different shades of growth Process after 2 hours synthesis.*

3.1 Characterization of GNBPs

UV-Vis is employed for a comprehensive examination of the optical characteristics exhibited by the samples, with wavelength analysis spanning from 200 to 1000 nm. Fig. 2 (a) illustrates the absorption spectrum of the seed, revealing a peak position at transversal Surface Plasmon Resonance (t-SPR) with the wavelength in the range 300 to 400 nm that surpasses the longitudinal SPR (l-SPR) in the range 700 to 800 nm. The comparable peak positions at t-SPR indicate uniform sizes of Au nanoseeds. Notably, a higher t-SPR signifies an elevated presence of decahedral impurities, while a lower l-SPR suggests a lower prevalence of bipyramidal structures [17]. Upon closer inspection as depicted in Fig. 2 (a), the 0.5-hour samples exhibited the smallest intensities in both t-SPR and l-SPR, registering as low as 0.4 and 0.04, respectively. In contrast, the 1-hour sample displayed two peaks at 0.42 and 0.04, with the highest intensities at t-SPR and l-SPR recorded as 0.49 and 0.09 in 2 hours. Remarkably, the progression from 0.5 hours to 2 hours showcased an increasing intensity of t-SPR, whereas the 3-hour samples experienced a decrease in t-SPR intensity. This phenomenon, identified as Ostwald ripening, is characterized by a temporal reduction in Au nanoseed quantity, accompanied by an enlargement in the size of larger particles [18].

The investigation proceeded with an examination of the optical properties of the synthesized GNBPs. Fig. 2 (b) presents the absorption spectrum during the growth phase in the formation of the as-synthesized GNBPs. the wavelength of t-SPR in the range 500 to 600 nm where l-SPR in the range 800 to 1000 nm. The results reveal a red shift in two absorption peaks, signifying changes in the optical characteristics. Following the initial 2 hours, the peak height experienced a reduction, accompanied by broadening, indicative of higher-order plasmon modes associated with larger particles [19]. The t-SPR peak correlates with the diameter of the GNBPs, while the l-SPR is linked to their aspect ratio [20], [21]. Corresponding to l-SPR, the absorption maximum peak undergoes a red shift as the aspect ratio increases, reflecting an increase in the diameter of the GNBPs [22]. Further analysis involves the recording of intensity values at t-SPR and l-SPR for all samples. At 0.5 hours, the recorded intensities are 1.3 and 2.33, respectively, whereas the 1-hour sample yields values of 1.37 and 2.37. Remarkably, the 2-hour sample attains the highest intensities, measuring 1.3 and 2.39, surpassing those of other durations. The 3-hour sample registers intensities of 1.22 and 2.1.

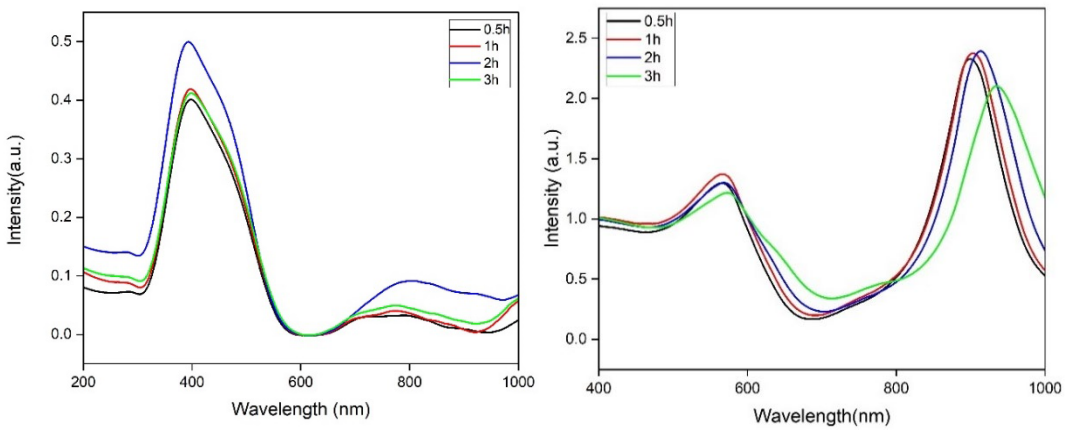

(a) **(b)**

Fig. 2 *Absorption spectrum with varying (a) seeding time and (b) the result synthesized GNBPs.*

Fig. 3 represents the FESEM result concerning morphological properties, while the corresponding records of average surface density and average aspect ratio are depicted in Fig. 4. The examination is conducted at magnifications of 50,000x and 100,000x to observe GNBPs and by-products formed on the substrate. The by-products are attributed to the rapid reduction of Au^{3+} to Au during the seeding process, hindering the atom's transition into specific facets and resulting in truncated shapes instead of GNBPs at various seeding durations [16]. The GNBPs' size exhibits an increment from 0.5 hours to 3 hours, with the maximum aspect ratio recorded as 3.27 ± 0.243 for the 3-hour sample and the minimum aspect ratio as 2.53 ± 0.149 for the 1-hour sample. Notably, the size of GNBPs, encompassing both length and diameter, demonstrates a correlation with surface density. The reduced rate of ascorbic acid dissociation, acting as a reduction agent, contributes to an incomplete reduction of Au3+ to Au, consequently diminishing GNBPs formation. Moreover, Au^{3+} not only undergoes reduction but also functions as an oxidant, leading to the etching of pre-existing GNBPs.

The 2-hour sample exhibits the highest surface density, registering 62.35±12.17%. In comparison, the 3-hour sample shows lower surface density of 20.02 ± 5.273 %. Conversely, the 0.5-hour and 1-hour samples demonstrate smaller surface densities, with values of 12.26 ± 3.729% and 16.38 ± 1.073 %, respectively.

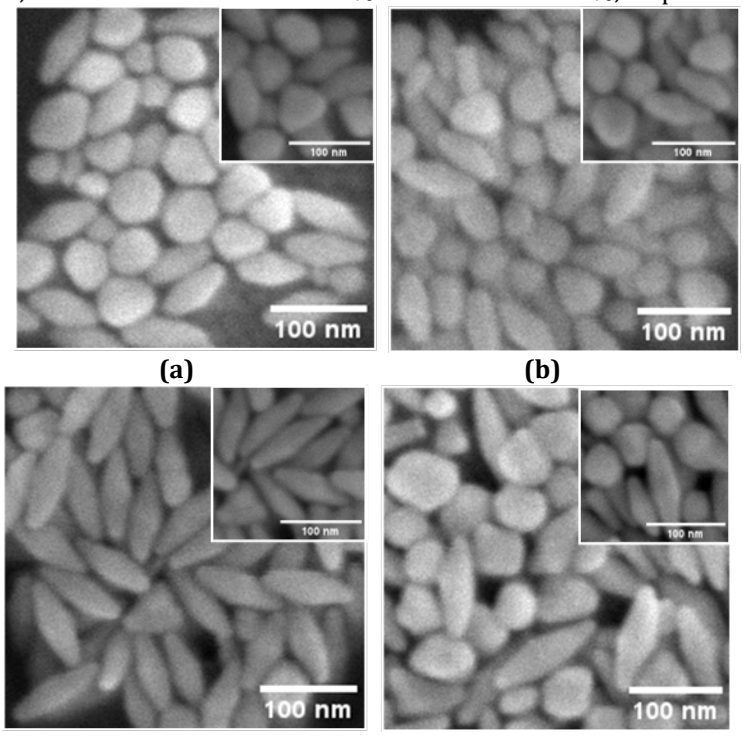

(a) **(b)**

(c) **(d)**

Fig. 3 *FESEM image of GNBPs with magnification 50,000x and inlet with magnification 100,000x (a) 0.5 hour (b) 1 hour (c) 2 hours (d) 3 hours.*

Evolution in Electrical and Electronic Engineering Vol. 5 No. 1 (2024) p. 497-503

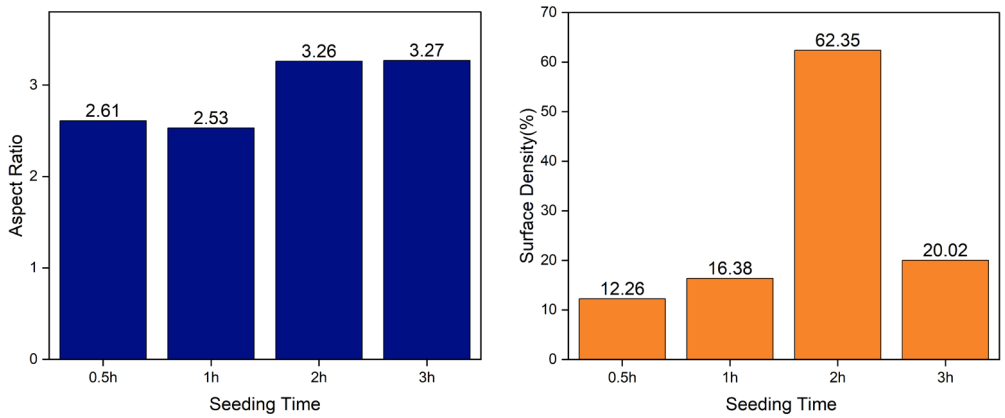

(a) **(b)**

Fig. 4 *Average with standard deviation error (a) aspect ratio and (b) surface density.*

3.2 Plasmonic Sensor Testing

Stability testing

To validate the stability of the plasmonic sensor, GNBPs from the 2-hour sample are selected as the sensing material and subjected to testing using deionized water (DIW) and a glucose solution with a concentration of 0.01 M. The t-SPR and l-SPR intensity of GNBPs is measured for 600 seconds non-stop. The stability responses of the GNBPs plasmonic sensors for t-SPR and l-SPR are illustrated in Fig. 5, representing (a) DIW and (b) glucose medium. The intensity values for DIW medium are 1.00 for t-SPR and 1.54 for l-SPR, while the corresponding values for glucose medium are 1.01 for t-SPR and 1.55 for l-SPR. As a comparison, the difference of both t-SPR and l-SPR bands between DIW and glucose is 0.01 where the higher t-SPR and l-SPR is in the presence of glucose 0.01 mol. The plasmonic sensor demonstrates good stability, exhibiting consistent intensity changes over time for both t-SPR and l-SPR peaks. Consequently, the results of the stability test affirm the promising practical applicability of the GNBP plasmonic sensor.

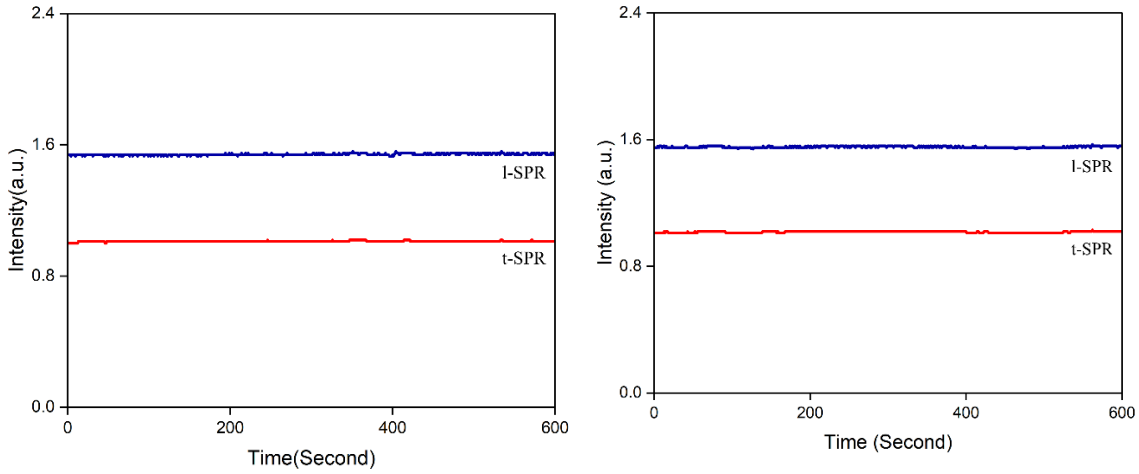

(a) **(b)**

Fig. 5 *Stability response of plasmonic sensor in (a) DIW and (b) glucose.*

4. Conclusion

The GNBPs are successfully synthesized utilizing the SMGM. The seeding time significantly influenced the growth of GNBPs, affecting the surface density and aspect ratio. After investigating the seeding time, a 2-hour seeding time was identified as the optimum time, with a surface density of 62.35 ± 12.17 % and an aspect ratio of 3.26 ± 0.099. Then, the GNBPs are tested as the sensing material to detect 0.01 M through the plasmonic sensor system. The plasmonic sensor setup consisted of five components: a light source, sensor chamber, fiber optic, spectrometer, and computer with Ocean View software. Then, the stability and selectivity are investigated in this work to obtain the plasmonic sensor performances. The plasmonic sensor exhibits good stability with a low change in intensity value over 600 seconds non-stop for both t-SPR and l-SPR towards DIW and glucose medium.

Acknowledgement

This research was supported by the Ministry of Higher Education (MOHE) through the Fundamental Research Grant Scheme (FRGS/1/2023/STG05/UTHM/02/3). The author also thanks Microelectronics and Nanotechnology – Shamsuddin Research Centre (MiNT-SRC), Universiti Tun Hussein Malaysia, for providing the laboratory facilities.

Conflict of Interest

Authors declare that there is no conflict of interests regarding the publication of the paper.

Author Contribution

The authors attest to having sole responsibility for the following: planning and designing the study, data collection, analysis and interpretation of the outcomes, and paper writing.

References

[1] A. Majdalawieh, M. C. Kanan, O. El-Kadri, and S. M. Kanan, "Recent advances in gold and silver nanoparticles: Synthesis and applications," *J. Nanosci. Nanotechnol.*, vol. 14, no. 7, pp. 4757–4780, 2014, doi: 10.1166/jnn.2014.9526.

[2] T. Taufikurohmah, I. G. M. Sanjaya, and A. Syahrani, "Nanogold synthesis using matrix mono glyceryl stearate as antiaging compounds in modern cosmetics," *J. Mater. Sci. Eng. A*, vol. 1, no. 6A, p. 857, 2011.

[3] X. Chen, Q. W. Li, and X. M. Wang, "Gold nanostructures for bioimaging, drug delivery and therapeutics," in *Precious metals for biomedical applications*, Elsevier, 2014, pp. 163–176. doi: 10.1533/9780857099051.2.163.

[4] E. C. Dreaden, A. M. Alkilany, X. Huang, C. J. Murphy, and M. A. El-Sayed, "The golden age: gold nanoparticles for biomedicine," *Chem. Soc. Rev.*, vol. 41, no. 7, pp. 2740–2779, 2012, doi: 10.1039%2Fc1cs15237h.

[5] N. Elahi, M. Kamali, and M. H. Baghersad, "Recent biomedical applications of gold nanoparticles: A review," *Talanta*, vol. 184, pp. 537–556, 2018, doi: 10.1016/j.talanta.2018.02.088.

[6] J. Wang *et al.*, "Gold nanobipyramid-loaded black phosphorus nanosheets for plasmon-enhanced photodynamic and photothermal therapy of deep-seated orthotopic lung tumors," *Acta Biomater.*, vol. 107, pp. 260–271, 2020, doi: 10.1016/j.actbio.2020.03.001.

[7] S. Nafisah *et al.*, "Improved sensitivity and selectivity of direct localized surface plasmon resonance sensor using gold nanobipyramids for glyphosate detection," *IEEE Sens. J.*, vol. 20, no. 5, pp. 2378–2389, 2020, doi: 10.1109/JSEN.2019.2953928.

[8] T. H. Chow, N. Li, X. Bai, X. Zhuo, L. Shao, and J. Wang, "Gold nanobipyramids: An emerging and versatile type of plasmonic nanoparticles," *Acc. Chem. Res.*, vol. 52, no. 8, pp. 2136–2146, 2019, doi: 10.1021/acs.accounts.9b00230.

[9] A. V Kabashin *et al.*, "Plasmonic nanorod metamaterials for biosensing," *Nat. Mater.*, vol. 8, no. 11, pp. 867–871, 2009, doi: 10.1038/nmat2546.

[10] S. Eustis and M. A. El-Sayed, "Why gold nanoparticles are more precious than pretty gold: noble metal surface plasmon resonance and its enhancement of the radiative and nonradiative properties of nanocrystals of different shapes," *Chem. Soc. Rev.*, vol. 35, no. 3, pp. 209–217, 2006.

[11] X. Huang, S. Neretina, and M. A. El-Sayed, "Gold nanorods: from synthesis and properties to biological and biomedical applications," *Adv. Mater.*, vol. 21, no. 48, pp. 4880–4910, 2009, doi: 10.1002/adma.200802789.

[12] M. Morsin, M. M. Salleh, M. Z. Sahdan, and F. Mahmud, "Effect of seeding time on the formation of gold nanoplates," *Int. J. Integr. Eng.*, vol. 9, no. 2, pp. 27–30, 2017.

[13] N. Z. A. Md Shah, M. Morsin, R. Sanudin, N. L. Razali, S. Nafisah, and C. F. Soon, "Effects of growth solutions ageing time to the formation of gold nanorods via two-step approach for plasmonic applications," *Plasmonics*, vol. 15, no. 4, pp. 923–932, 2020, doi: 10.1007/s11468-019-01098-2.

[14] M. Zaitoun, M. Ghanem, and S. Harphoush, "Sugars: Types and their functional properties in food and human health," *Int. J. Public Heal. Res.*, vol. 6, no. 4, pp. 93–99, 2018.

[15] S. Chaudhary, V. P. Jain, and G. Jaiswar, "The composition of polysaccharides: monosaccharides and binding, group decorating, polysaccharides chains," in *Innovation in Nano-Polysaccharides for Eco-sustainability*, Elsevier, 2022, pp. 83–118. doi: 10.1016/B978-0-12-823439-6.00005-2.

[16] Suratun Nafisah, Marlia Morsin, Iwantono Iwantono, Rahmat Sanudin, Zainiharyati Mohd Zain, Lusiana Satria, Nur Liyana Razali, & Dedi Mardiansyah. "Growth time dependency on the formation of gold nanobipyramids for efficient detection towards chlorpyrifos-based LSPR sensor," 2023, no. *289*, pp. 171270–171270. doi.org/10.1016/j.ijleo.2023.171270

[17] T. V. K. Ngo, P. T. Huynh, A. T. K. Nguyen, G. D. Nguyen, and V. Q. Lam, "Synthesis of gold nanobipyramids

by seed-mediated method and antibacterial activities," *Commun. Phys.*, vol. 28, no. 2, p. 179, 2018, doi: 10.15625/0868-3166/28/2/10846.

[18] T. Kajita and M. Oyama, "Tuning of nanostructures of gold nanoparticles on indium tin oxide surfaces using a seed-mediated growth method," *J. Electroanal. Chem.*, vol. 656, no. 1–2, pp. 264–268, 2011, doi: 10.1016/j.jelechem.2010.10.020.

[19] K. G. Stamplecoskie, J. C. Scaiano, V. S. Tiwari, and H. Anis, "Optimal size of silver nanoparticles for surface-enhanced Raman spectroscopy," *J. Phys. Chem. C*, vol. 115, no. 5, pp. 1403–1409, 2011, doi: 10.1021/jp106666t.

[20] S. L. Smitha, K. G. Gopchandran, N. Smijesh, and R. Philip, "Size-dependent optical properties of Au nanorods," *Prog. Nat. Sci. Mater. Int.*, vol. 23, no. 1, pp. 36–43, 2013, doi: 10.1016/j.pnsc.2013.01.005.

[21] A. Moores and F. Goettmann, "The plasmon band in noble metal nanoparticles: an introduction to theory and applications," *New J. Chem.*, vol. 30, no. 8, pp. 1121–1132, 2006, doi: 10.1039/b604038c.

[22] P. F. Fox, "Lactose: Chemistry and properties," *Adv. Dairy Chem. Vol. 3 Lact. Water, Salts Minor Const.*, pp. 1–15, 2009.

[23] S. S. Dhondge, D. W. Deshmukh, L. J. Paliwal, and P. N. Dahasahasra, "The study of molecular interactions of ascorbic acid and sodium ascorbate with water at temperatures (278.15, 288.15 and 298.15) K," *J. Chem. Thermodyn.*, vol. 67, pp. 217–226, 2013, doi: 10.1016/j.jct.2013.08.016.

[24] X. Huang and M. A. El-Sayed, "Gold nanoparticles: Optical properties and implementations in cancer diagnosis and photothermal therapy," Journal of Advanced Research, vol. 1, no. 1, pp. 13–28, 2010.

[25] Santosh Kumar Meena, Lerouge, F., Baldeck, P. L., Andraud, C., Garavelli, M., Parola, S. Rivalta, I. "On the origin of controlled anisotropic growth of monodisperse gold nanobipyramids." Nanoscale, vol. 13 , pp. 15292– 15300, doi: org/10.1039/d1nr01768c, 2021.

[26] Sweeney, C. M., Stender, C. L., Nehl, C. L., Hasan, W., Shuford, K. L., & Odom, T. W. Optical Properties of Tipless Gold Nanopyramids. Small, vol. 7, pp. 2032–2036, doi: org/10.1002/smll.201100758,2013